Volume 1, Number 3

JPCR | JOURNAL OF PEDIATRIC CASE REPORTS

A MULTIDISCIPLINARY JOURNAL OF CASE REPORTS

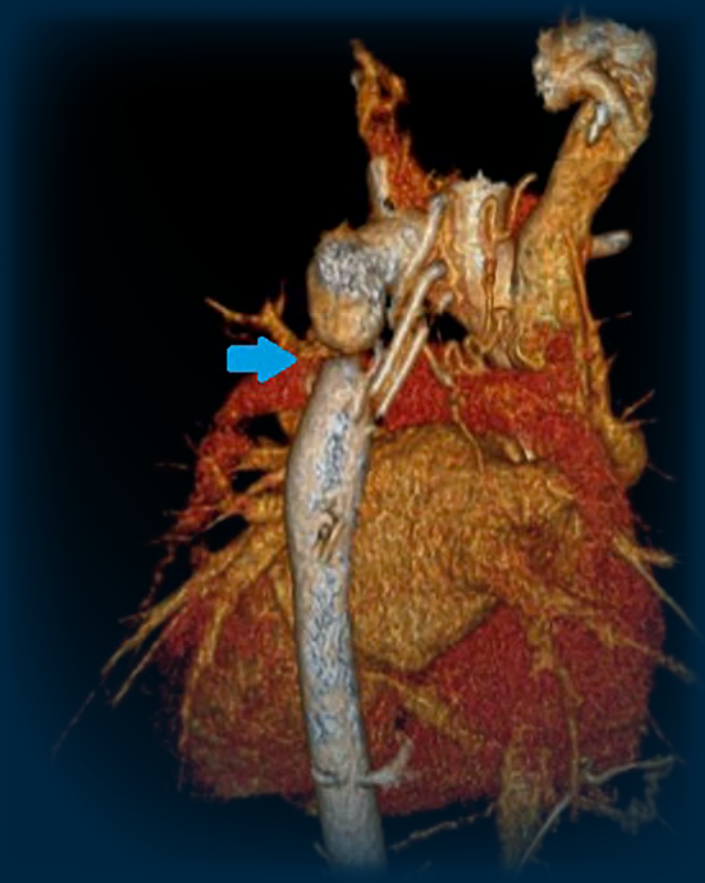

Button Battery Ingestion

Pulmonary Interstitial Glycogenosis

Juvenile Dermatomyositis

Hemolytic Uremic Syndrome

Leak from Duplicated Thoracic Duct Treated with Embolization

Pulmonary Aspergilloma

www.journalofpediatriccasereports.com

JPCR | JOURNAL OF PEDIATRIC CASE REPORTS

A MULTIDISCIPLINARY JOURNAL OF CASE REPORTS

Anderson Publishing, Ltd
180 Glenside Avenue,
Scotch Plains, NJ 07076
Tel: 908-271-8644

VOLUME 1 NUMBER 3

Button Battery Ingestion

Brandon T. Klor, BS; Richard B. Towbin, MD; Carrie M. Schaefer, MD; Alexander J. Towbin, MD

Abstract

Button battery ingestion is an increasingly common cause of pediatric emergency department visits. Diagnosis is primarily made through radiographic evaluation, with anterior-posterior and lateral views distinguishing button batteries from other radiopaque foreign bodies. While most patients recover without complications, the caustic nature of modern lithium batteries necessitates careful evaluation and close follow-up to prevent potentially fatal outcomes. High-risk cases include children under 6 years of age, ingestion of batteries 20 mm or larger, and esophageal impaction, all of which require urgent intervention and monitoring.

Keywords: gastrointestinal, eophagus, trauma, ingestion

Case Summary

A toddler presented with 1 day of non-bilious vomiting. She was initially diagnosed with a viral illness, but her symptoms progressed to include persistent emesis, fever, and decreased oral intake. Due to these ongoing concerns, she was brought to the emergency department where a chest radiograph was obtained.

Imaging Findings

Chest radiograph (Figure 1) demonstrated a button battery lodged within the proximal esophagus at the level of the aortic arch. Following endoscopic removal, a chest CT (Figure 2) revealed residual battery fragments but no vascular injury. An esophagram (Figure 3) performed 2 weeks later showed mild irregularity of the proximal esophagus at the site of impaction.

Figure 1. (A) Frontal and (B) lateral chest radiographs showing a button battery (arrow) lodged within the proximal esophagus at the level of the aortic arch. The battery demonstrates an irregular margin, suggesting prolonged impaction and early degradation.

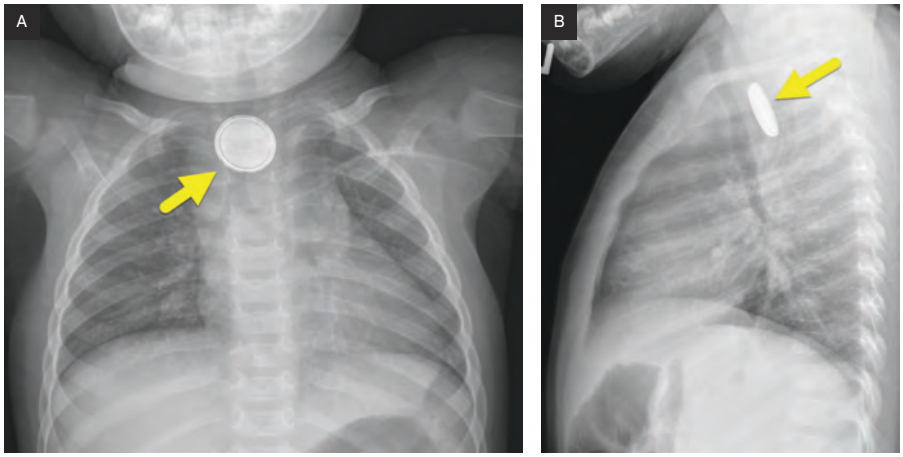

Diagnosis

Button battery ingestion.

The imaging differential diagnosis includes button battery ingestion, coin ingestion, and magnet ingestion.

Discussion

Button battery ingestion is a medical emergency due to its potential for severe and life-threatening complications. When lodged in the esophagus, button batteries can generate a localized electrical current, leading to mucosal injury, liquefactive necrosis, and perforation within hours. Additionally, leakage of alkaline or lithium-containing substances can cause further tissue damage, increasing the risk of fistula formation, mediastinitis, and

Affiliations: University of Arizona College of Medicine- Phoenix, Phoenix, Arizona (Klor); Department of Radiology, Phoenix Children's Hospital, Phoenix, Arizona (RB Towbin, Schaefer); Department of Radiology, Cincinnati Children's Hospital, University of Cincinnati College of Medicine, Cincinnati, Ohio (AJ Towbin).
Disclosures: The authors have no conflicts of interest to disclose. None of the authors received outside funding for the production of this original manuscript and no part of this article has been previously published elsewhere.

https://doi.org/10.37549/JPCR-26-0088

Figure 2. Axial CT images of the chest in (A) soft tissue and (B) bone windows, along with (C) coronal CT reconstruction, showing residual battery fragments (arrow) at the prior site of impaction. No adjacent aortic wall irregularity is identified.

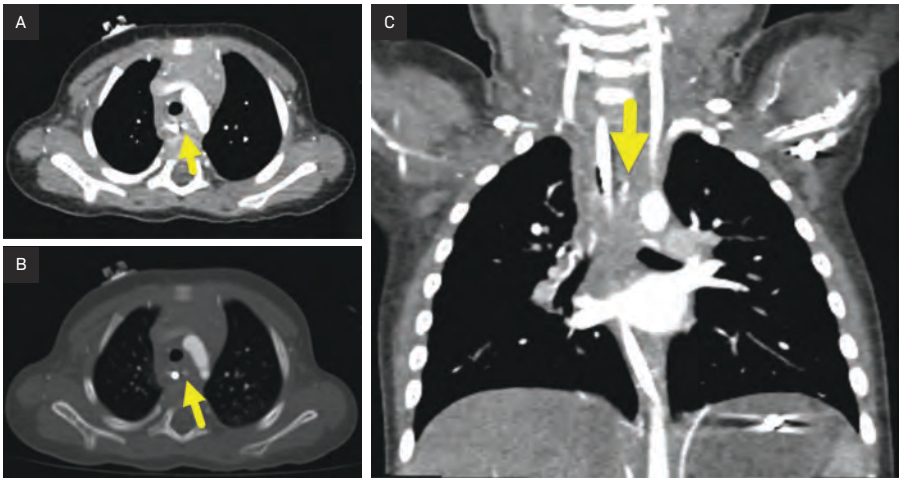

even fatal vascular injury. Given these serious consequences, rapid identification and removal are critical to prevent irreversible injury.

The prevalence of button battery ingestions has increased significantly in recent decades. In 1995, only 0.14% of emergency department visits for foreign body ingestions in children under 6 years old were attributed to batteries.[1] By 2015, this number had risen to 8.4%, with 85.9% of identified batteries being button batteries.[1] Two key factors have contributed to this trend: the larger diameters of modern button batteries, which increase the risk of esophageal impaction, and the conversion to lithium cells, which are more caustic to human tissues.[2]

In cases of witnessed button battery ingestion, patients often present with acute gastrointestinal symptoms, including vomiting, dysphagia, and abdominal pain, or with respiratory symptoms such as cough, stridor, or shortness of breath. In unwitnessed ingestions, symptoms may appear later, often manifesting as gastrointestinal hemorrhage or constitutional symptoms such as fever or weight loss.[3]

Given the severity of button battery ingestion, identifying patients at highest risk for complications is critical. The most vulnerable populations include children under 6 years of age and those who ingest lithium batteries larger than 20 mm in diameter.[2,4] Once a battery becomes lodged, it can rapidly induce tissue damage, with the gastrointestinal tract being the most affected system. Complications range from ulceration (22.1%) and perforation (18.1%) to more severe injuries such as tracheoesophageal fistulas (14.6%), strictures or obstruction (13.7%), and tissue necrosis (4.9%)—the majority of which involve the esophagus. In the most severe cases, vascular involvement occurs in 6% of complications, as the battery erodes through the gastrointestinal wall into adjacent arteries or veins. This can result in catastrophic hemorrhage due to rapid vascular extravasation and exsanguination, making it one of the most feared and fatal consequences of button battery ingestion.[4]

Given the potential for life-threatening complications, rapid and accurate diagnosis of button battery ingestion is essential. The initial imaging evaluation includes anterior-posterior and lateral chest radiographs.[3] On frontal radiographs, button batteries exhibit a "halo" or "double rim" sign, where the larger cathode portion forms the outer ring, and the radiopaque central circle represents both the cathode and anode. On lateral radiographs, this translates to a "step-off" sign, where the anode protrudes slightly from the cathode, producing a characteristic step-like appearance.

Figure 3. Lateral image from an upper gastrointestinal examination demonstrating focal irregularity (arrow) of the proximal esophagus at the site of prior battery impaction.

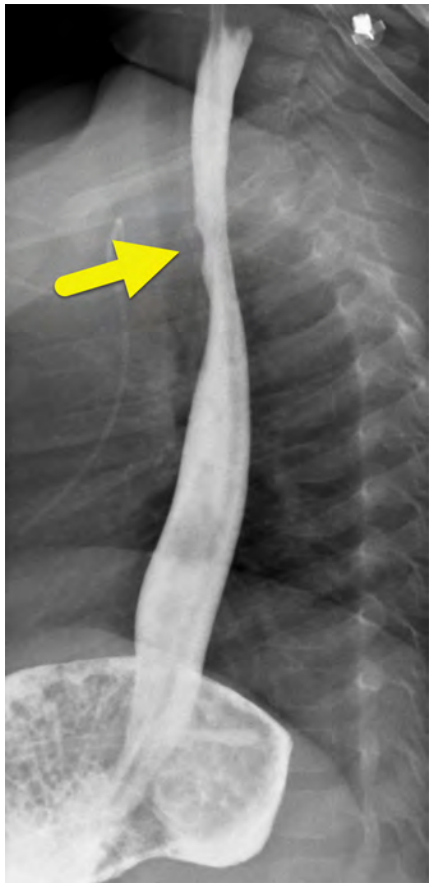

The radiographic appearance of button batteries can sometimes be mimicked by other radiopaque objects, such as stacked coins. Batteries smaller than 20 mm may not display the halo sign due to variations in battery morphology, but the step-off sign remains a reliable indicator for identifying button batteries of all sizes. Therefore, when observed, the step-off sign should raise strong suspicion for button battery ingestion.[5]

Serial CT or MRI is used to assess the extent of soft tissue injury following button battery removal and to monitor resolution.[3,6] Both modalities may

demonstrate soft tissue edema at the site of impaction, which can take weeks to resolve. MRI may also reveal blooming artifact, resulting from a combination of hydroxide ions generated during the initial caustic injury and hemosiderin deposition.[6] Additionally, CT may detect residual metallic fragments from the battery surface.

When interpreting radiologic studies, it is particularly important to evaluate tissue at the anode contact site, as this location carries the highest risk of injury, especially in the esophagus. This occurs because the negative pole of the battery generates hydroxide ions, leading to localized corrosive tissue damage.[3,4,6] In cases of button battery ingestion with suspected hemorrhage, CTA is used to assess the adjacent aorta.[7] Key imaging findings of aortic injury include periaortic edema, aortic wall thickening, and pseudoaneurysm formation.

Most patients with button battery ingestion have a favorable prognosis, with a low overall complication rate of 0.165 %.[4] However, when complications do occur, they can be life-threatening, particularly in cases of esophageal impaction. Impacted batteries require urgent endoscopic removal to prevent progressive tissue damage and fatal hemorrhage.[2,4]

Conclusion

Button battery ingestion is an increasingly common cause of pediatric emergency department visits. Diagnosis is primarily made through radiographic evaluation, with anterior-posterior and lateral views distinguishing button batteries from other radiopaque foreign bodies.

While most patients recover without complications, the caustic nature of modern lithium batteries necessitates careful evaluation and close follow-up to prevent potentially fatal outcomes. High-risk cases include children under 6 years of age, ingestion of batteries 20 mm or larger, and esophageal impaction, all of which require urgent intervention and monitoring.

References

1) Orsagh-Yentis D, McAdams RJ, Roberts KJ, McKenzie LB. Foreign-body ingestions of young children treated in US emergency departments: 1995-2015. *Pediatrics*. 2019;143(5):e20181988. doi:10.1542/peds.2018-1988

2) Kramer RE, Lerner DG, Lin T, et al. Management of ingested foreign bodies in children: a clinical report of the NASPGHAN endoscopy committee. *J Pediatr Gastroenterol Nutr*. 2015;60(4):562-574. doi:10.1097/MPG.0000000000000729

3) Mubarak A, Benninga MA, Broekaert I, et al. Diagnosis, management, and prevention of button battery ingestion in childhood: a European society for paediatric gastroenterology hepatology and nutrition position paper. *J Pediatr Gastroenterol Nutr*. 2021;73(1):129-136. doi:10.1097/MPG.0000000000003048

4) Varga Á, Kovács T, Saxena AK. Analysis of complications after button battery ingestion in children. *Pediatr Emerg Care*. 2018;34(6):443-446. doi:10.1097/PEC.0000000000001413

5) Meyer TJ, Grunz J-P, Taeger J, et al. Systematic analysis of button batteries', euro coins', and disk magnets' radiographic characteristics and the implications for the differential diagnosis of round radiopaque foreign bodies in the esophagus. *Int J Pediatr Otorhinolaryngol*. 2020;132:109917. doi:10.1016/j.ijporl.2020.109917

6) Grey NEO, Malone LJ, Miller AL, et al. Magnetic resonance imaging findings following button battery ingestion. *Pediatr Radiol*. 2021;51(10):1856-1866. doi:10.1007/s00247-021-05085-w

7) Demiroren K. Management of gastrointestinal foreign bodies with brief review of the guidelines. *Pediatr Gastroenterol Hepatol Nutr*. 2023;26(1):1-14. doi:10.5223/pghn.2023.26.1.1

Pulmonary Interstitial Glycogenosis

Janice Wang, BA; Richard B. Towbin, MD; Carrie M. Schaefer, MD; Alexander J. Towbin, MD

Abstract

Pulmonary interstitial glycogenosis (PIG) is a rare interstitial lung disease that presents in neonates with rapidly progressive respiratory distress. Because there are no specific clinical, radiologic, or genetic markers for the disease, diagnosis relies on lung biopsy. Prognosis depends on disease context: isolated PIG is typically associated with favorable outcomes, whereas cases with concurrent pulmonary or cardiovascular abnormalities may have a more complicated clinical course. Treatment generally includes corticosteroids and supportive care, tailored to the severity of respiratory symptoms and any underlying conditions.

Keywords: thorax, lung, congenital, cause unknown

Case Summary

An infant born at 34 weeks started grunting in the neonatal intensive care unit and ultimately required continuous positive airway pressure ventilation, exogenous surfactant, and intubation. After extubating, the patient required oxygen.

Imaging Findings

Radiograph (Figure 1) and chest CT (Figure 2) were obtained at 6 weeks of age. Both show diffuse ground-glass opacity and small cystic spaces in the posterior aspect of the lungs.

Diagnosis

Pulmonary interstitial glycogenosis (PIG).

Differential diagnosis includes bronchopulmonary dysplasia (chronic lung disease of prematurity), neuroendocrine hyperplasia of infancy, surfactant dysfunction disorders, and glycogen storage diseases.

Discussion

PIG, previously termed *cellular interstitial pneumonitis* or *histiocytoid pneumonia*, is a rare form of neonatal interstitial lung disease that typically affects infants younger than 6 months of age.[1] The exact cause remains unknown, but PIG is thought to be a congenital abnormality resulting from abnormal alveolar growth or impaired lung remodeling, leading to restricted differentiation of pulmonary interstitial fibroblasts.[2,3] This process results in the accumulation of glycogen within the interstitial cells of the lung.

PIG remains poorly understood, with most of the literature limited to case reports. Its reported incidence ranges from 0.1 to 16 cases per 100,000 children per year, with a slight male predominance.[4] PIG occurs in both term and preterm infants and is frequently associated with other congenital lung abnormalities and cardiovascular disease, including pulmonary hypertension, structural heart defects, alveolar simplification, and extrapulmonary conditions such as Noonan syndrome, inborn errors of metabolism, and Trisomy 21.[1,2,5,6] PIG may also present as an isolated finding, in which case the clinical course is often favorable.[2]

Clinically, neonates and infants with PIG present with rapidly progressive respiratory distress, tachypnea, and hypoxemia in the absence of infection.[7,8] After an initial period of stability, respiratory function may deteriorate,

Figure 1. Frontal chest radiograph showing diffuse ground-glass opacity.

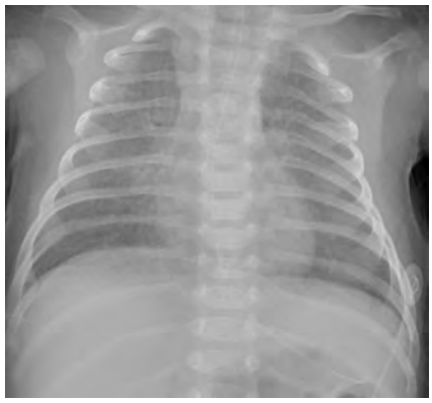

Affiliations: Kansas City University College of Osteopathic Medicine, Kansas City, Missouri (Wang); Department of Radiology, Phoenix Children's Hospital, Phoenix, Arizona (RB Towbin, Schaefer); Department of Radiology, Cincinnati Children's Hospital, University of Cincinnati College of Medicine, Cincinnati, Ohio (AJ Towbin).

Disclosures: The authors have no conflicts of interest to disclose. None of the authors received outside funding for the production of this original manuscript and no part of this article has been previously published elsewhere.

https://doi.org/10.37549/JPCR-26-0089

Figure 2. Axial images from chest CT obtained at the level of the (A) carina, (B) main pulmonary artery, and (C) lung bases showing diffuse ground-glass opacity and small cystic spaces (arrowheads) in the posterior lungs.

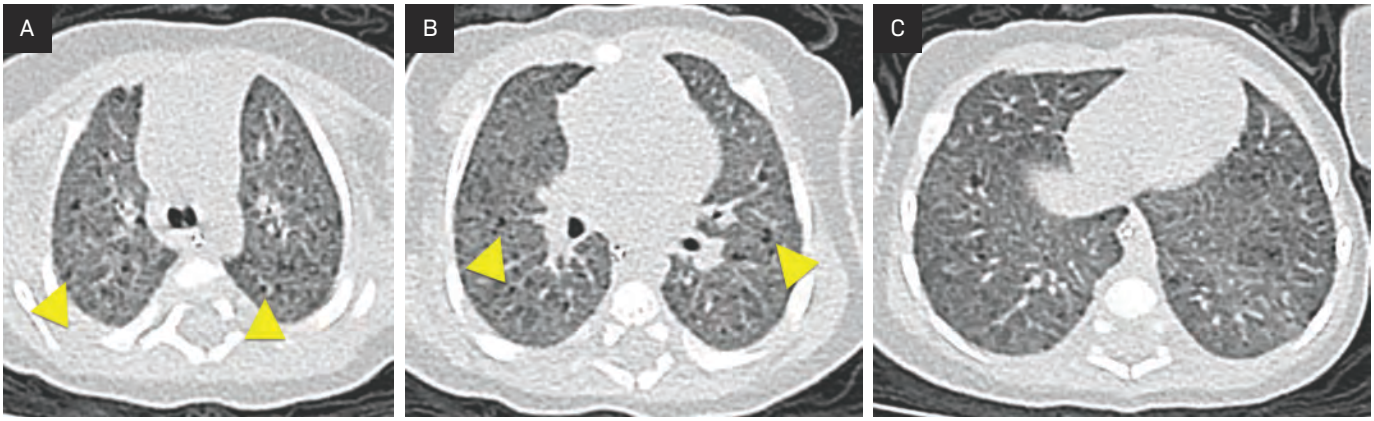

requiring varying levels of support. When PIG is suspected, the gold standard for diagnosis is lung biopsy, which reveals expansion of the interstitium by spindle-shaped mesenchymal cells with pale cytoplasm containing glycogen.[2,3]

High-resolution chest CT in PIG typically demonstrates features of interstitial lung disease, though no uniform imaging pattern has been established. The most common findings include diffuse ground-glass opacities and cystic lucencies, which are most pronounced in the posterior lungs.[5,9] These cystic lucencies are not true cysts but instead correspond to areas of alveolar simplification.[2] Less frequent imaging findings in PIG include interlobular septal thickening and architectural distortion. The extent of imaging findings does not correlate with the degree of lung growth abnormality or clinical outcome.[2]

There is no established consensus for the treatment of PIG. Systemic corticosteroids, typically administered as monthly pulses, are commonly used with anecdotal reports of clinical improvement.[5,10] Although PIG lacks active inflammation, corticosteroids are thought to promote lung maturation, potentially by accelerating apoptosis of lipofibroblasts.[2,5] Additional supportive therapies include oxygen supplementation and pulmonary rehabilitation in milder cases, while severe cases may require extracorporeal membrane oxygenation or even lung transplantation.[1,5]

Overall, prognosis depends largely on the extent of lung development and the presence of associated comorbidities. Patients with isolated PIG tend to experience significant clinical improvement and a favorable outcome, whereas those with underlying abnormalities have a more variable prognosis.[1,5]

Conclusion

PIG is a rare interstitial lung disease that presents in neonates with rapidly progressive respiratory distress. Because there are no specific clinical, radiologic, or genetic markers for the disease, diagnosis relies on lung biopsy. Prognosis depends on disease context: isolated PIG is typically associated with favorable outcomes, whereas cases with concurrent pulmonary or cardiovascular abnormalities may have a more complicated clinical course. Treatment generally includes corticosteroids and supportive care, tailored to the severity of respiratory symptoms and any underlying conditions.

References

1) Deutsch GH, Cortes-Santiago N. Acquired and idiopathic disorders in neonates and young children. In: *Pulmonary Pathology*. Elsevier. 2025:62-82. doi:10.1016/B978-0-323-93548-7.00005-2

2) Sardón O, Torrent-Vernetta A, Rovira-Amigo S, et al. Isolated pulmonary interstitial glycogenosis associated with alveolar growth abnormalities: a long-term follow-up study. *Pediatr Pulmonol*. 2019;54(6):837-846. doi:10.1002/ppul.24324

3) Deutsch GH, Young LR. Lipofibroblast phenotype in pulmonary interstitial glycogenosis. *Am J Respir Crit Care Med*. 2016;193(6):694-696. doi:10.1164/rccm.201509-1809LE

4) Das S, Langston C, Fan LL. Interstitial lung disease in children. *Curr Opin Pediatr*. 2011;23(3):325-331. doi:10.1097/MOP.0b013e3283464a37

5) Liptzin DR, Baker CD, Darst JR, et al. Pulmonary interstitial glycogenosis: diagnostic evaluation and clinical course. *Pediatr Pulmonol*. 2018;53(12):1651-1658. doi:10.1002/ppul.24123

6) Cutz E, Chami R, Dell S, Langer J, Manson D. Pulmonary interstitial glycogenosis associated with a spectrum of neonatal pulmonary disorders. *Hum Pathol*. 2017;68:154-165. doi:10.1016/j.humpath.2017.06.026

7) Griese M, Seidl E. Persistent tachypnea of infancy, neuroendocrine cell hyperplasia of infancy, and pulmonary interstitial glycogenosis: "A3-specific conditions of undefined etiology". *Pediatr Pulmonol*. 2024;59(10):2702-2707. doi:10.1002/ppul.27102

8) Seidl E, Carlens J, Reu S, et al. Pulmonary interstitial glycogenosis - a systematic analysis of new cases. *Respir Med*. 2018;140:11-20. doi:10.1016/j.rmed.2018.05.009

9) Weinman JP, White CJ, Liptzin DR, et al. High-resolution CT findings of pulmonary interstitial glycogenosis. *Pediatr Radiol*. 2018;48(8):1066-1072. doi:10.1007/s00247-018-4138-4

10) Hamberger E, Yu Y, Choi HJ. Pulmonary interstitial glycogenosis in two neonates: early recognition and use of corticosteroids. *Respir Med Case Rep*. 2024;48:101990. doi:10.1016/j.rmcr.2024.101990

Juvenile Dermatomyositis

Abdelfatah Fatah, BS; Richard B. Towbin, MD; Carrie M. Schaefer, MD; Alexander J. Towbin, MD

Abstract

Juvenile dermatomyositis is a rare autoimmune inflammatory myopathy characterized by progressive proximal muscle weakness and distinctive skin manifestations. Imaging, particularly MRI, plays a crucial role in diagnosis and monitoring, detecting muscle edema, inflammation, and chronic atrophy. Calcinosis is a common complication, particularly in children, and serves as a marker of disease progression. Treatment primarily involves glucocorticoids, with immunosuppressive agents used to minimize long-term steroid exposure. While remission is achievable, ongoing management is necessary to prevent relapses and complications.

Keywords: musculoskeletal, myositis, skin, chronic, cause unknown

Case Summary

A child with long-standing undertreated dermatomyositis was imaged to assess soft tissue complications.

Imaging Findings

Radiographs (Figure 1) of the upper and lower extremity and CT of the pelvis (Figure 2) show extensive subcutaneous soft tissue calcifications (arrows). MRI at the level of the acetabulum and lower extremity showing calcification and muscle involvement. (Figure 3)

Diagnosis

Dermatomyositis.

The clinical differential diagnosis includes various types of myopathies, including mitochondrial myopathies, infectious and inflammatory myopathies, autoimmune necrotic myopathies plus Duchenne or Becker muscular dystrophy, systemic lupus erythematosus, and juvenile idiopathic arthritis. Polymyositis, systemic sclerosis, and mixed connective tissue disease may have similar imaging profiles.

Discussion

Dermatomyositis is a rare autoimmune inflammatory muscle disorder of unknown cause that primarily affects skeletal muscle and skin. The incidence is estimated at 9.63 per million adults and 1.9-4.1 per million children.[1,2] When dermatomyositis occurs in children, it is referred to as juvenile dermatomyositis. The juvenile form has distinct clinical and laboratory findings compared with the adult form. Characteristic features include progressive muscle weakness and skin rashes, often accompanied by systemic symptoms such as anorexia, pain, fever, irritability, and general deterioration.[3] Compared with adult-onset disease, juvenile dermatomyositis is associated with a lower malignancy risk and a more consistent response to therapy.

Juvenile dermatomyositis is classified as an inflammatory myopathy, a group of uncommon conditions characterized by chronic muscle inflammation and weakness.[1] While myopathy is a broad term encompassing various muscle disorders, juvenile dermatomyositis can be distinguished through a combination of clinical symptoms, laboratory findings, histopathologic evaluation, and imaging.

Juvenile dermatomyositis typically presents in children 5-14 years of age with a subacute onset of muscle weakness, primarily affecting proximal muscles symmetrically, like adult dermatomyositis. Routine activities such as brushing teeth, climbing stairs, lifting objects, and dressing become progressively difficult.

While distal muscle weakness, pain, and stiffness are rare in adults, they occur more frequently in children, making it more challenging to distinguish juvenile dermatomyositis from juvenile idiopathic arthritis.[4] Dysphagia or dysphonia is reported in 18-20% of patients.[5] On examination, proximal muscle weakness is the most prominent finding, while muscle tenderness is typically mild, and distal strength remains preserved unless the disease is severe and longstanding.

When a muscle biopsy is performed, findings diagnostic of dermatomyositis include perivascular and perimysial inflammatory infiltrates composed of

Affiliations: Texas College of Osteopathic Medicine, Fort Worth, Texas (Fatah); Department of Radiology, Phoenix Children's Hospital, Phoenix, Arizona (RB Towbin, Schaefer); Department of Radiology, Cincinnati Children's Hospital, University of Cincinnati College of Medicine, Ohio (AJ Towbin).
Disclosures: The authors have no conflicts of interest to disclose. None of the authors received outside funding for the production of this original manuscript and no part of this article has been previously published elsewhere.

https://doi.org/10.37549/JPCR-26-0090

Figure 1. Radiographs of the (A) right upper arm, (B) right femur, and (C) right knee showing sheet-like dystrophic calcifications (arrows) within the soft tissues.

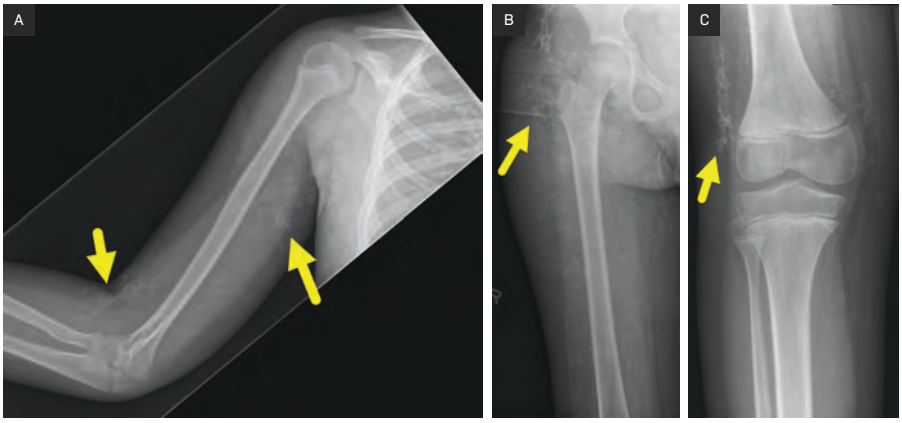

Figure 2. Axial CT image of the pelvis showing dystrophic calcification (arrows) at the subcutaneous fat-muscle interface.

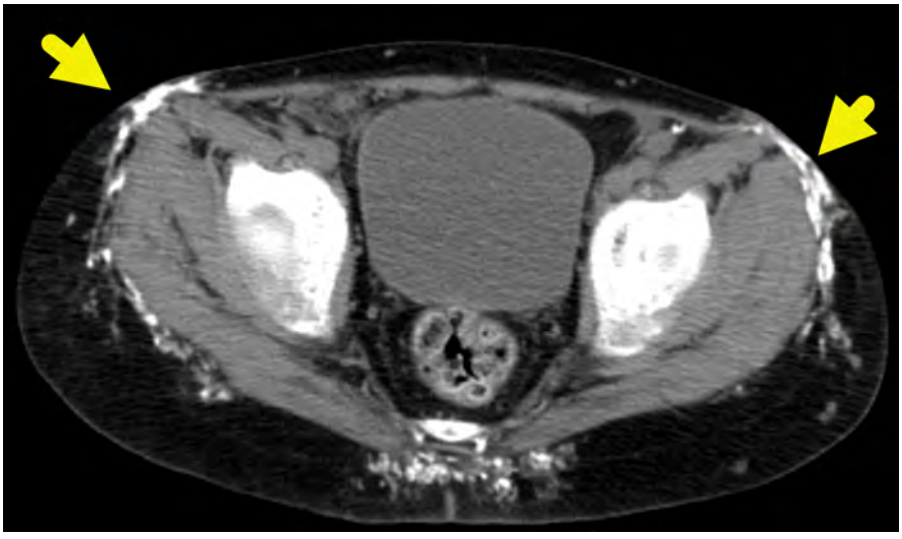

B cells, CD4+ T helper cells, macrophages, and plasmacytoid dendritic cells, along with perifascicular atrophy and microangiopathy.[1]

In both children and adults with dermatomyositis, characteristic skin lesions often precede muscle weakness. In up to 40% of patients, skin involvement is the sole presenting feature, a condition known as dermatomyositis sine myositis.

Dermatomyositis is associated with distinctive cutaneous manifestations, including the heliotrope rash—a violaceous discoloration of the eyelids—and Gottron's papules, which are pathognomonic for the disease.[6] Gottron's papules present as violaceous papules over the metacarpophalangeal joints, proximal and distal interphalangeal joints of the hands, and sometimes on the extensor surfaces of the elbows and knees. Additional findings include periungual erythema with telangiectasia, cuticular hypertrophy, facial edema, and a V-shaped erythematous patch over the anterior neck and upper chest. Raynaud phenomenon may also be present.[3]

Histopathologic findings in dermatomyositis closely resemble those seen in systemic lupus erythematosus. Key features include vacuolar changes in the basal layer, increased lymphocytic infiltration, and elevated mucin deposition within the dermis. Due to overlapping clinical and histologic features with other autoimmune diseases, a comprehensive evaluation is necessary before establishing a definitive diagnosis.[1]

Although the diagnosis of dermatomyositis is primarily based on clinical, biochemical, and histopathological findings, imaging plays an important role in disease evaluation. It aids in identifying calcinosis, detecting muscle changes in the active disease phase, diagnosing complications, ruling out other conditions, guiding biopsies, and monitoring disease progression during follow-up.[7]

Calcinosis, or dystrophic soft tissue calcifications, develops in 30-70% of children with juvenile dermatomyositis and typically occurs in the chronic phase of the disease. These calcium deposits are more common in children and adolescents and form in areas of skin, subcutaneous tissue, fascial planes, and muscle necrosis. In juvenile dermatomyositis, calcinosis can develop within 6 months of disease onset and progressively worsens over time. Because the extent of calcinosis correlates with disease duration, it serves as an important marker of disease progression, alongside muscle weakness and elevated creatine kinase and lactate dehydrogenase levels.[8] MRI is the preferred imaging modality for diagnosing and monitoring dermatomyositis, offering detailed visualization of both superficial and deep tissues. Unlike US, MRI is not operator-dependent, provides a wider field of view, and is unaffected by superficial calcifications, making it particularly valuable for evaluating deeper structures.[9]

MRI is highly sensitive for detecting acute inflammatory edema, fatty replacement, and muscle atrophy. T2-weighted and short tau inversion recovery sequences highlight muscle edema, which appears hyperintense due to increased water content, a hallmark of active muscle inflammation in dermatomyositis. T1-weighted imaging is useful for assessing muscle atrophy, with

Figure 3. (A) Axial and (B) coronal short tau inversion recovery MR images of the lower extremities demonstrating mild increased T2 signal within the thigh musculature, most prominently at the myofascial junctions.

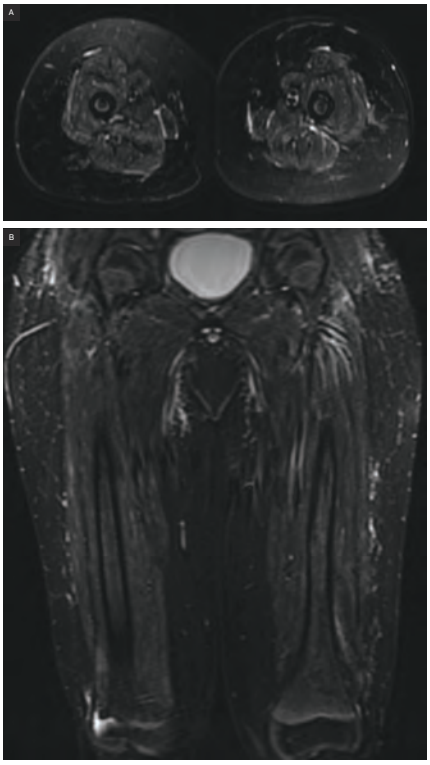

affected muscle appearing hyperintense, reflecting muscle loss and fatty infiltration. Post-contrast MRI highlights areas of active inflammation, with findings ranging from minimal skin or subcutaneous fat involvement to widespread muscle and myofascial disease.[10]

US is a valuable tool in assessing disease activity, distinguishing between active and chronic disease, detecting subclinical involvement, and confirming remission.[10] Increased muscle echogenicity suggests inflammation and edema, while a heterogeneous echotexture of the muscle reflects varying degrees of inflammation and fibrosis. In early disease, muscles appear swollen and thickened due to active inflammation. In chronic dermatomyositis, the muscle becomes thin and atrophic, reflecting prolonged inflammation and muscle damage.[10]

While dermatomyositis lacks a curative treatment, extended periods of remission are attainable. With appropriate therapy, disease-related mortality in juvenile dermatomyositis is 2-3%. Glucocorticoids remain the first-line treatment, with prednisone being the most used corticosteroid. Corticosteroid-sparing agents, such as methotrexate or azathioprine, are often introduced to minimize long-term steroid use. In children with severe muscle weakness, high-dose prednisone may be initiated for rapid disease control. However, prolonged glucocorticoid use carries risks, including weight gain, behavioral changes, hypertension, increased infection risk, and impaired bone growth.

Because methotrexate takes approximately 3 months to become effective, it is not the preferred choice in patients requiring immediate disease control. Once clinical improvement is observed, glucocorticoids are gradually tapered to the lowest effective dose to maintain disease control and normalize enzyme levels. Biologic therapies, such as rituximab and anti-tumor necrosis factor agents, are reserved for refractory cases and are not routinely used.[6]

Conclusion

Juvenile dermatomyositis is a rare autoimmune inflammatory myopathy characterized by progressive proximal muscle weakness and distinctive skin manifestations. Imaging, particularly MRI, plays a crucial role in diagnosis and monitoring, detecting muscle edema, inflammation, and chronic atrophy. Calcinosis is a common complication, particularly in children, and serves as a marker of disease progression. Treatment primarily involves glucocorticoids, with immunosuppressive agents used to minimize long-term steroid exposure. While remission is achievable, ongoing management is necessary to prevent relapses and complications.

References

1) Qudsiya Z, Dermatomyositis WM. Dermatomyositis. In: *StatPearls* [Internet]. StatPearls Publishing. 2023. https://www.ncbi.nlm.nih.gov/books/NBK558917/

2) Tansley SL, McHugh NJ, Wedderburn LR. Adult and juvenile dermatomyositis: are the distinct clinical features explained by our current understanding of serological subgroups and pathogenic mechanisms? *Arthritis Res Ther*. 2013;15(2):211. doi:10.1186/ar4198

3) Gara S, Jamil RT, Muse ME, et al. Juvenile dermatomyositis. In: *StatPearls* [Internet]. StatPearls Publishing. https://www.ncbi.nlm.nih.gov/books/NBK534236/

4) Boyarchuk O, Kuka A, Yuryk I. Clinical and autoantibody phenotypes of juvenile dermatomyositis. *Reumatologia*. 2022;60(4):281-291. doi:10.5114/reum.2022.119045

5) Kwon KMM, Lee JSM, Kim YHM. A case report of life-threatening acute dysphagia in dermatomyositis: challenges in diagnosis and treatment. *Medicine*. 2018;97(17):e0508. doi:10.1097/MD.0000000000010508

6) Sudoł-Szopińska I, Jacques T, Gietka P, Cotten A. Imaging in dermatomyositis in adults and children. *J Ultrason*. 2020;20(80):e36-e42. doi:10.15557/JoU.2020.0007

7) Sanyal S, Atwal SS, Mondal D, Garga UC. Radiographic patterns of soft tissue calcinosis in juvenile dermatomyositis and its clinical implications. *J Clin Diagn Res*. 2014;8(12):RD08-RD11. doi:10.7860/JCDR/2014/10787.5321

8) Davuluri S, Duvvuri B, Lood C, Faghihi-Kashani S, Chung L. Calcinosis in dermatomyositis: origins and possible therapeutic avenues. *Best Pract Res Clin Rheumatol*. 2022;36(2):101768. doi:10.1016/j.berh.2022.101768

9) Spalkit S, Sinha A, Prakash M, Sandhu MS. Dermatomyositis: patterns of MRI findings in muscles, fascia and skin of pelvis and thigh. *Eur J Radiol*. 2021;141:109812. doi:10.1016/j.ejrad.2021.109812

10) Kasapcopur O, Barut K, Avar PO, et al. Juvenile dermatomyositis: clinical features, laboratory findings, treatment modalities and disease course (a single center experience). *Pediatr Rheumatol*. 2014;12(s1):P276. doi:10.1186/1546-0096-12-S1-P276

https://doi.org/10.37549/JPCR-26-0090

Hemolytic Uremic Syndrome

Irene H. Jo, BA; Richard B. Towbin, MD; Carrie M. Schaefer, MD; Alexander J. Towbin, MD

Abstract

Hemolytic uremic syndrome (HUS) is a thrombotic microangiopathy defined by the triad of renal failure, hemolytic anemia, and thrombocytopenia. It is a leading cause of acute kidney injury in young children. HUS is now classified by etiology rather than clinical features, with Shiga toxin-producing *Escherichia coli* accounting for most pediatric cases. Atypical HUS, most often due to complement dysregulation, is less common and carries a higher risk for chronic renal impairment. Diagnosis is clinical, supported by gastrointestinal symptoms and characteristic laboratory findings. Imaging plays an important role in evaluating complications and guiding treatment. Renal US can help assess disease severity, while neuroimaging is used in patients with suspected central nervous system involvement. Management is primarily supportive, with early hydration and dialysis when indicated. Outcomes depend on the underlying etiology and severity of organ involvement, with neurologic and cardiac complications being the primary drivers of mortality.

Keywords: renal, vascular, chronic kidney disease

Case Summary

A toddler presented with 2 days of diarrhea and vomiting without fever. Stool cultures confirmed infection with *Escherichia coli*.

Imaging Findings

Bowel US (Figure 1) showed diffuse bowel wall thickening, bowel hyperemia, and mild ascites. The kidneys were enlarged and echogenic. Subsequent abdominal CT (Figure 2) showed similar findings. The kidneys appeared enlarged with abnormal decreased cortical enhancement.

Diagnosis

Hemolytic uremic syndrome (HUS).

The differential diagnosis includes thrombotic thrombocytopenic purpura, disseminated intravascular coagulation, malignant hypertension, juvenile-onset, and systemic lupus erythematosus.

Figure 1. (A) Transverse color Doppler US image of the bowel in the right lower quadrant showing diffuse bowel wall thickening (arrow), bowel hyperemia, and mild ascites (arrowhead). (B) Longitudinal image of the right kidney showing it to be enlarged and diffusely echogenic.

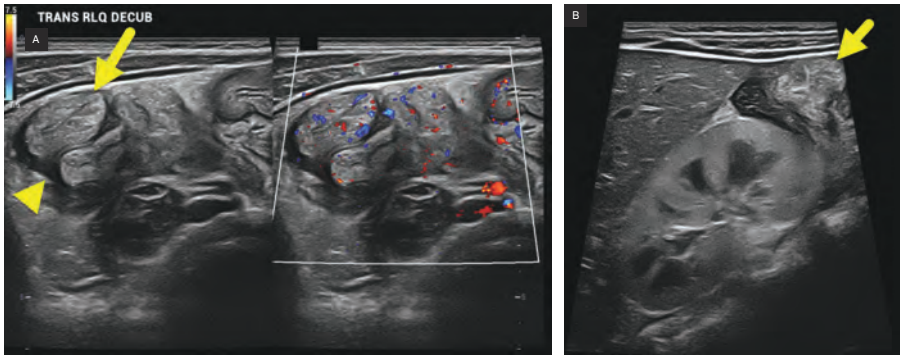

Discussion

HUS is a thrombotic microangiopathy characterized by a clinical triad of renal failure, hemolytic anemia, and thrombocytopenia. It is a major cause of acute kidney injury and acquired chronic kidney disease in children under 5 years of age.[1]

Historically, HUS was classified by the presence or absence of diarrhea: "typical" or "diarrhea-positive" HUS, and "atypical" or "diarrhea-negative" HUS.[2] However, recent studies have shown that atypical HUS (aHUS) can present with diarrhea in up to 30% of cases.[3] As a result, a classification based on etiology is now preferred. Shiga toxin-producing *Escherichia coli* hemolytic uremic syndrome (STEC-HUS) accounts for 85-90% of pediatric cases.[2,3]

Affiliations: University of Arizona College of Medicine-Phoenix Campus, Phoenix, Arizona (Jo); Department of Radiology, Phoenix Children's Hospital, Phoenix, Arizona (RB Towbin, Schaefer); Department of Radiology, Cincinnati Children's Hospital, University of Cincinnati College of Medicine, Cincinnati, Ohio (AJ Towbin).

Disclosures: The authors have no conflicts of interest to disclose. None of the authors received outside funding for the production of this original manuscript and no part of this article has been previously published elsewhere.

https://doi.org/10.37549/JPCR-26-0091

Figure 2. (A) Axial and (B) coronal CT images of the abdomen showing diffuse bowel wall thickening (arrows), mild ascites (arrowhead), and abnormal enhancement of the diffusely enlarged kidneys.

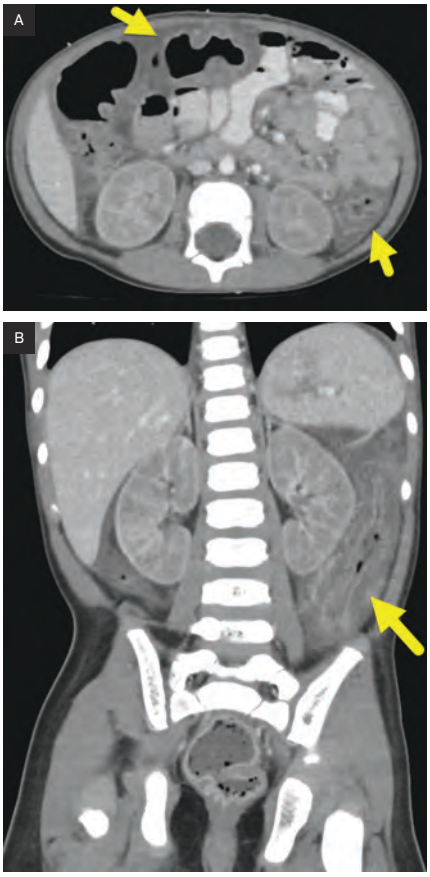

Approximately 15% of children infected with STEC develop HUS. The Shiga toxin binds to globotriaosylceramide receptors on renal endothelial cells, initiating inflammation, endothelial damage, and microvascular thrombosis.[4,5]

In contrast, aHUS is primarily a result of dysregulation of the alternative complement pathway. It accounts for 5-10% of HUS cases and may be either genetic or sporadic. Mutations in complement regulatory genes are identified in about 50% of patients with aHUS.[5] Additional rare variants include *Streptococcus pneumoniae*-associated HUS and secondary forms related to autoimmune diseases, transplants, or infections. Despite evolving classification schemes, inconsistency in terminology remains across the literature. aHUS usually presents with nonspecific symptoms such as fatigue, pallor, or somnolence that may progress to acute kidney injury. The risk of progression to end-stage kidney disease is high. Like HUS, aHUS demonstrates extrarenal findings and can present with diarrhea in about a third of cases.[6]

Epidemiologic patterns vary by geography and age.[2] Children have the highest incidence. In Europe and North America, STEC-HUS occurs at rates of 0.6-0.8 per 100,000 children under 15-18 years of age, and 1.9-2.9 per 100,000 in those under 3-5 years. Incidence in Latin America is approximately 10 times higher. In contrast, aHUS is rare, with an estimated incidence of 0.10-0.11 cases per million children.[7]

Diagnosis is clinical, supported by a history of gastrointestinal illness and laboratory findings consistent with the HUS triad. Patients with STEC-HUS typically develop watery, bloody diarrhea 3-8 days after exposure to contaminated food.[2] Associated symptoms include abdominal pain, vomiting, and hypertension. Renal involvement ranges from hematuria and proteinuria to oliguria and acute kidney failure, with approximately 20% requiring dialysis.[8]

Central nervous system involvement occurs in 20-50% of patients and is the most serious complication leading to increased mortality and long-term neurologic deficits.[4] Neurologic symptoms include seizures, irritability, altered mental status, and focal deficits. Other organ systems may also be affected, with potential complications including gastrointestinal injury, cardiac ischemia, diabetes mellitus, and hepatomegaly.[2] The overall mortality rate for HUS is about 5%, primarily due to central nervous system and cardiac complications.

Laboratory evaluation typically reveals hemolytic anemia, thrombocytopenia, and elevated creatinine. Schistocytes may be seen on peripheral smear. Stool culture or PCR for *E. coli* O157:H7 can support a diagnosis of STEC-HUS, although serum anti-O157 antibody may be more sensitive.[4]

Imaging is used to help support the diagnosis, identify potential complications, and assess disease severity. Chest radiography may help assess for pulmonary edema and cardiac enlargement. Echocardiography is indicated when cardiac dysfunction is suspected.[9]

Renal US is helpful during the prodromal phase. Resistive index (RI) and kidney size are useful in assessing disease severity. Rink et al. found that patients with HUS had elevated RI (mean 0.87±0.10) and increased kidney volume (mean 177.4% of age-adjusted normal) at disease onset. Patients requiring dialysis had larger kidneys than those who did not.[10]

Neuroimaging is used to evaluate central nervous system complications. Noncontrast CT is typically used to exclude hemorrhage or infarction. MRI provides greater sensitivity for cytotoxic edema and is useful for assessing disease severity and prognosis. Bilateral T2 and diffusion-weighted hyperintensities in the basal ganglia, thalami, and white matter are common findings.[4,11] These changes are often reversible, although in severe cases they may predict poor neurologic outcomes.

Management is primarily supportive. Most patients require transfusion of volume-reduced, platelet-depleted red blood cells.[4] Early aggressive intravenous hydration (10 mL/kg/hour of 0.9% saline for 3 hours) can reduce dialysis requirements, hospital stay, and the risk of central nervous system injury.[12] About half of the STEC-HUS patients require dialysis. End-stage renal disease is more common in aHUS and may necessitate kidney transplantation. Antibiotics and antidiarrheal agents are avoided in STEC-HUS due to the risk of increased Shiga toxin release. In contrast, antibiotics

are indicated for *S. pneumoniae*-associated HUS.

Conclusion

HUS is a thrombotic microangiopathy defined by the triad of renal failure, hemolytic anemia, and thrombocytopenia. It is a leading cause of acute kidney injury in young children. HUS is now classified by etiology rather than clinical features, with STEC accounting for the majority of pediatric cases. aHUS, most often due to complement dysregulation, is less common and carries a higher risk for chronic renal impairment.

Diagnosis is clinical, supported by gastrointestinal symptoms and characteristic laboratory findings. Imaging plays an important role in evaluating complications and guiding treatment. Renal US can help assess disease severity, while neuroimaging is used in patients with suspected central nervous system involvement. Management is primarily supportive, with early hydration and dialysis when indicated. Outcomes depend on the underlying etiology and severity of organ involvement, with neurologic and cardiac complications being the primary drivers of mortality.

References

1) Grisaru S. Management of hemolytic-uremic syndrome in children. *Int J Nephrol Renovasc Dis*. 2014;7:231-239. doi:10.2147/IJNRD.S41837

2) Gülhan B, Özaltın F. Hemolytic uremic syndrome in children. *Turk Arch Pediatr*. 2021;56(5):415-422. doi:10.5152/TurkArchPediatr.2021.21128

3) Bhandari J, Rout P, Sedhai YR. Hemolytic uremic syndrome. In: *StatPearls*. StatPearls Publishing. 2023.

4) Boyer O, Niaudet P. Hemolytic-uremic syndrome in children. *Pediatr Clin North Am*. 2022;69(6):1181-1197. doi:10.1016/j.pcl.2022.07.006

5) Petruzziello-Pellegrini TN, Marsden PA. Shiga toxin-associated hemolytic uremic syndrome: advances in pathogenesis and therapeutics. *Curr Opin Nephrol Hypertens*. 2012;21(4):433-440. doi:10.1097/MNH.0b013e328354a62e

6) Jokiranta TS. HUS and atypical HUS. *Blood*. 2017;129(21):2847-2856. doi:10.1182/blood-2016-11-709865

7) Raina R, Krishnappa V, Blaha T, et al. Atypical hemolytic-uremic syndrome: an update on pathophysiology, diagnosis, and treatment. *Ther Apher Dial*. 2018;23(1):4-21. doi:10.1111/1744-9987.12763

8) Rivetti G, Gizzone P, Petrone D, et al. Acute kidney injury in children: a focus for the general pediatrician. *Children*. 2024;11(8):1004. doi:10.3390/children11081004

9) Kim E, Kim SY. Multiple extrarenal manifestations in hemolytic uremic syndrome: a case report. *Korean J Pediatr*. 2007;50(12):1261. doi:10.3345/kjp.2007.50.12.1261

10) Rink L, Finkelberg I, Kreuzer M, et al. Ultrasound analysis of different forms of hemolytic uremic syndrome in children. *Front Pediatr*. 2024;12:1433812. doi:10.3389/fped.2024.1433812

11) Mansour MA, Khalil DF, Hasham MA, et al. Hemolytic uremic syndrome with central nervous system manifestations, a case report and literature review. *Radiol Case Rep*. 2023;18(6):2268-2273. doi:10.1016/j.radcr.2023.02.035

12) Bilkis MD, Bonany P. Hydration in hemolytic uremic syndrome. *Arch Argent Pediatr*. 2021;119(1):62-66. doi:10.5546/aap.2021.eng.62

https://doi.org/10.37549/JPCR-26-0091

Leak from Duplicated Thoracic Duct Treated with Embolization

Haley P. Baier, BS; Richard B. Towbin, MD; Carrie M. Schaefer, MD; Alexander J. Towbin, MD

Abstract

Injury to the thoracic duct leads to the leakage of chyle into the pleural space causing a chylothorax. The most common cause of chylothorax in children is injury from cardiac surgery when the mediastinum is dissected. It is important to diagnose and localize the chyle leak. Today, intranodal lymphangiography with MRI is the gold standard for diagnostic imaging and guidance of therapy. Medical management is often the initial therapy. If unsuccessful, image-guided embolization is the initial treatment of choice and is an effective treatment for a persistent chylothorax after unsuccessful medical management.

Keywords: thorax, trauma, lymphatic, lymphatic embolization

Case Summary

A teenaged male with hypertensive crisis was found to have an aortic interruption. Within days following repair of the aortic interruption, there was development of a left chylous pleural effusion. A dynamic contrast-enhanced MR lymphangiogram was performed, demonstrating localized accumulation of contrast near the thoracic duct at the aortic arch level and accumulation of contrast in the left pleural effusion. Afterward, an MR lymphangiogram was performed, with transabdominal cannulation of the thoracic duct, and embolization of the leaking duplicated thoracic duct.

Imaging Findings

A 3D CTA of the chest with a posterior view demonstrated an interrupted thoracic aorta (Figure 1). A dynamic contrast-enhanced MR lymphangiogram 33 minutes later showed the thoracic duct (TD) (Figure 2A) and accumulation of contrast near the TD at the T3 level (blue arrow, Figure 2B). Transabdominal TD access with contrast injection demonstrated duplication of the TD (Figure 3A), with leakage of contrast from the left-sided duplication. The TD was cannulated with a microcatheter. The catheter tip was positioned in the inferior-most aspect of the left-sided TD duplication. There was successful coil embolization with resolution of the leak.

Diagnosis

Duplicated TD with associated laceration and chylothorax.

The differential diagnosis includes hemothorax, exudative pleural effusion, pseudochylothorax (cholesterol effusion), empyema, parapneumonic pleural effusion, and rarely rheumatoid and lipoid pleural effusions.

Figure 1. 3D CTA of the chest with a posterior view demonstrating a severe coarctation/interruption of the aorta (blue arrow).

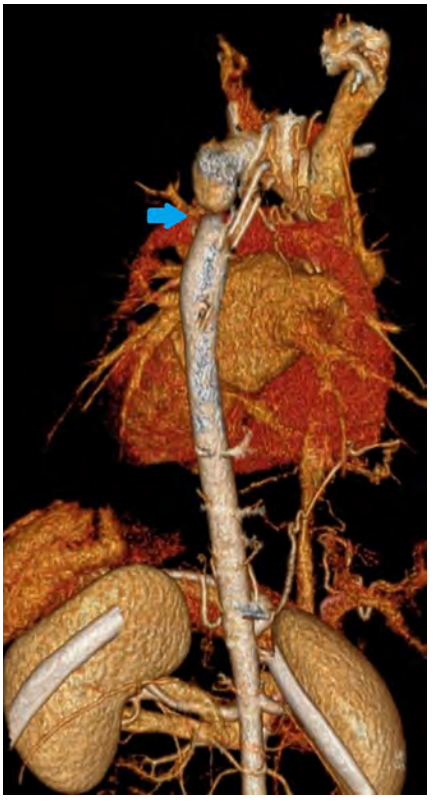

Discussion

Chyle is a milky fluid that is formed in the small intestines and consists of fats

Affiliations: Kansas City University College of Medicine, Kansas City, Missouri (Baier); Department of Radiology, Phoenix Children's Hospital, Phoenix, Arizona (RB Towbin, Schaefer); Department of Radiology, Cincinnati Children's Hospital, University of Cincinnati College of Medicine, Cincinnati, Ohio (AJ Towbin).
Disclosures: The authors have no conflicts of interest to disclose. None of the authors received outside funding for the production of this original manuscript and no part of this article has been previously published elsewhere.

https://doi.org/10.37549/JPCR-26-0092

Figure 2. (A, B) Dynamic contrast-enhanced MR lymphangiogram demonstrating visualization of the thoracic duct (TD) at 33 minutes (blue arrows, A) and accumulation of contrast near the TD at the T3 level (blue arrow, B).

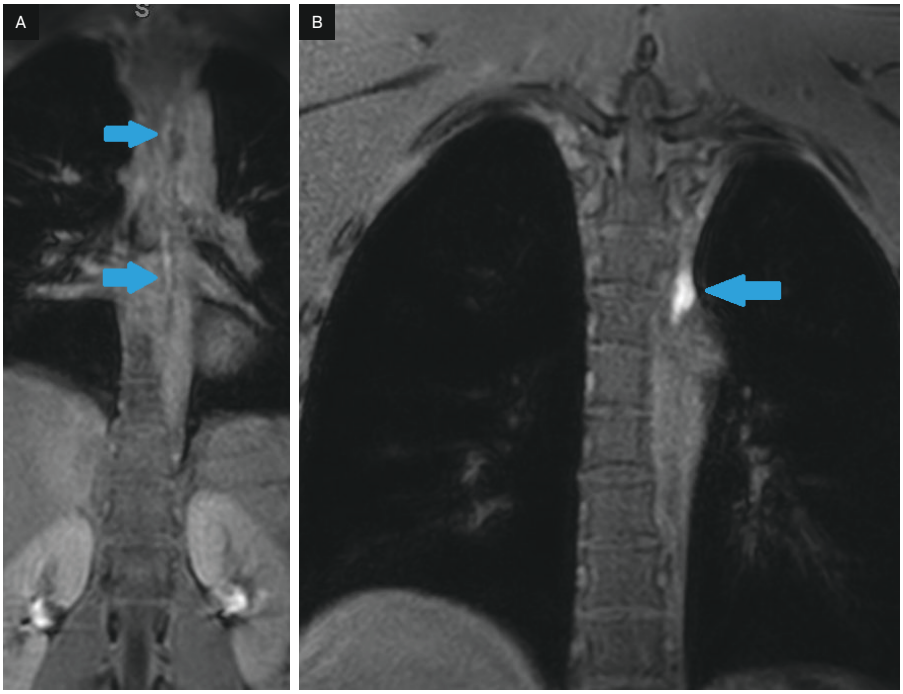

or free fatty acids. Normally lymph drains from the lacteals of the small intestines into the lymphatics. The lymphatic vessels drain chyle from the intestine and join with lymphatic fluid from the lower extremities flowing into the TD system, which ultimately drains approximately 75% of the lymph originating from the cisterna chyli and empties into the venous system at the junction of the left subclavian vein and left jugular vein.[1] The right lymphatic duct is smaller than the TD and drains about 25% of the lymphatic fluid originating from the right side of the head and neck, the right upper extremity, right thorax, and right breast. This duct independently drains into the right subclavian vein/internal jugular junction. The right duct can be injured in right-sided neck dissections or other trauma, presents with right-sided fluid collections, and occurs in about 0.75-8.9% of cases. The TD is the longest and largest lymphatic channel, which drains into the left subclavian vein. It courses through the trunk and may be affected by congenital anomalies and trauma, especially from surgical procedures. Anatomic variation can be found in nearly one-third of children, adding to the risk of surgical injury. A partial duplication of the TD occurs in about 15-20% of cases. TD duplication or triplication can also be seen. Chylothorax is a rare condition that results from TD damage, with chyle leakage from the lymphatic system into the pleural space.[2] As approximately 2.4 L of chyle is transported through the lymphatic system every day, damage to or rupture of the TD can give rise to a large and rapid accumulation of fluid in the pleural space.[2]

Clinical features of chylothorax depend on the rate of chyle loss as well as the concomitant effect of the etiology.[2] Rapid fluid loss is associated with hypovolemia and respiratory difficulty as the pleural space fills with fluid.[3] Prolonged chyle drainage can also impact immune function and result in impairment in both cell-mediated and humoral immunity.[3]

Chylothorax can be traumatic, spontaneous, and idiopathic. Traumatic chylothorax results from disruption of the right lymphatic duct or TD at any point along its course in the body cavity and mediastinum.[1] Postoperative chylothorax is the most common form of traumatic chylothorax in modern medicine.[1] In children, the most common causes of injury are cardiac surgery (0.2-2%) (Figure 1) and pediatric surgery, followed by injuries causing high intrathoracic pressure. The primary cause of spontaneous or nontraumatic chylothorax can arise from congenital, neoplastic, or infectious etiologies.[1] While esophageal resection is considered the most common iatrogenic cause in adults, case reports have also documented idiopathic chylothorax occurring during pregnancy, triggered by labor.[1] Iatrogenic causes of chylothorax in the pediatric population are usually the result of congenital lymphatic dysplasia, malformations, severe infection, and Turner and Noonan syndrome. Operative correction of an aortic coarctation was the most common single cause of a subsequent chylothorax.[4]

Investigation of suspected chylothorax begins with the confirmation of the diagnosis by fluid analysis, followed by the identification of the leakage point where possible.[2] On fluid analysis, usually the total lipid varies from 4 to 40 g/L and characteristically has a high triglyceride and a low cholesterol concentration.[4] MR lymphangiography (MRL) (Figure 2) and nuclear medicine lymphangiography (NML) are the key imaging modalities used for diagnosis and localization of chyle leaks.[3] For NML, the usual site of tracer injection for lymphatic imaging is the web space between the first and second toes.[5] Despite a resurgence in pedal lymphangiography, it remains technically challenging and time-consuming, and NML has lower anatomic resolution.[6] Currently, the lymphatic system is most frequently accessed via inguinal lymph nodes (intranodal lymphangiography [INL]).[6] INL with lipiodol followed by MRI is the diagnostic tool of choice. Lipiodol also has therapeutic value for closing a chyle leak.[7] When a TD fistula is present, MRL can demonstrate its location by visualization of contrast extravasation from the duct with pooling in the

Figure 3. (A-C) Transabdominal thoracic duct access with contrast injection demonstrating duplication of the thoracic duct (TD) in (A) (blue arrow), with leakage of contrast from the left-sided duplication (green arrowhead). (B) The microcatheter tip is in the inferior-most aspect of the left-sided TD duplication, and there is contrast exiting the caudad aspect of the duplicated TD (green arrowhead). Successful coil embolization of the leaking duplicated TD with cessation of contrast leak (blue arrow) can be seen.

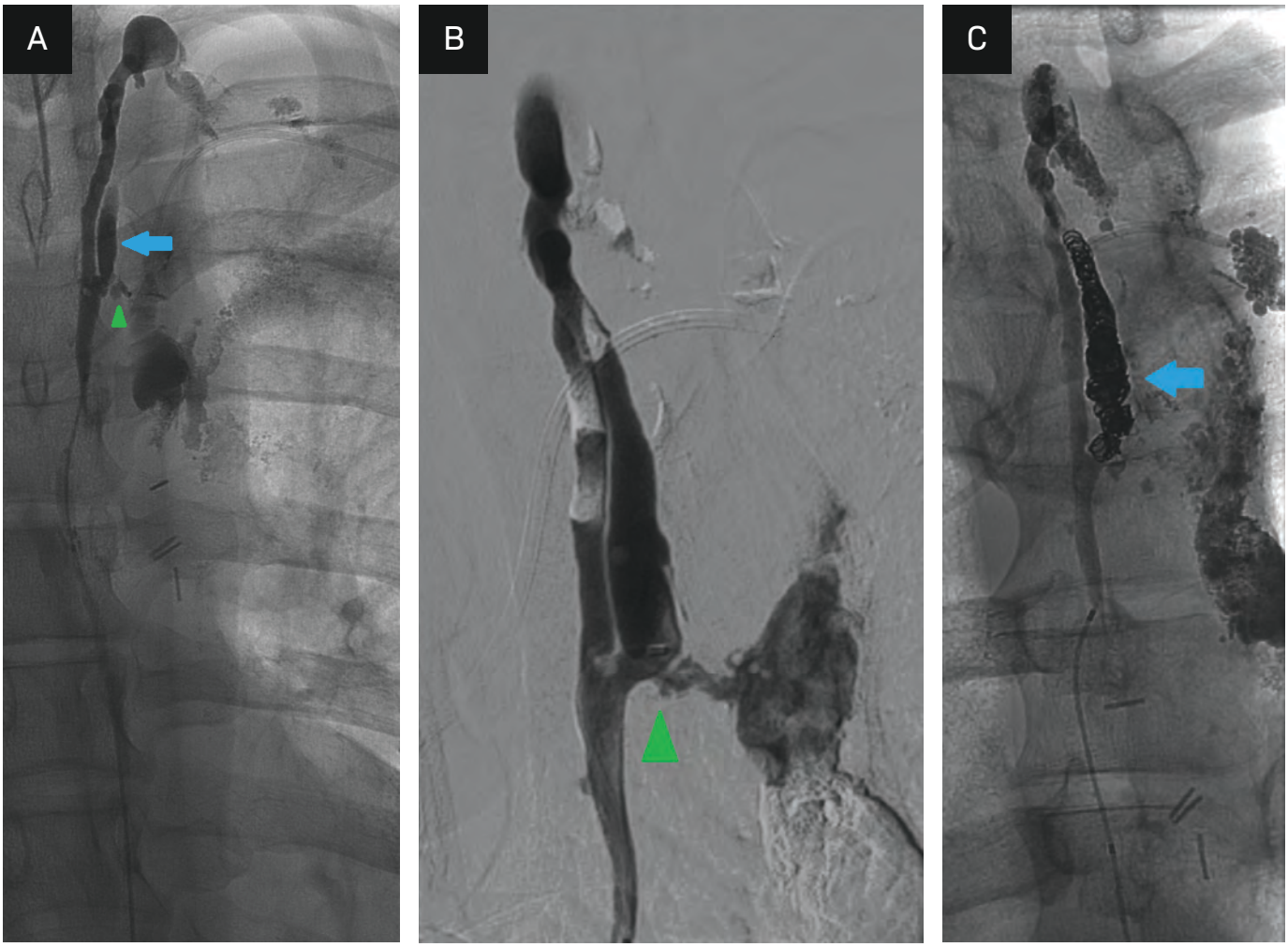

adjacent pleural space.[3] A post-lymphangiography noncontrast CT may be a useful adjunct and can precisely localize the source and location of the chyle leak.[3] However, MRL using heavily T2-weighted images has demonstrated greater sensitivity in identifying the cisterna chyli compared with lymphangiography or CT and is currently the diagnostic modality of choice.[8]

Chylothorax after congenital heart surgery occurs in approximately 2-5% of cases and can be associated with significant morbidity, especially in the repair of single ventricles.[9] Traditionally, treatment options included diet modification and octreotide infusion as conservative management.[9] The management of chylous effusions requires the maintenance of nutrition, reduction of flow in TD lymph, and maintenance of full expansion of the affected lung.[4] This may be accomplished via thoracentesis or chest tube placement.[10] Dietary modifications can help reduce the volume of chyle production and allow the site of injury to heal.[10] Medium-chain triglycerides by mouth resolve approximately 50% of congenital or traumatic chylothoraces.[2] Somatostatins constrict smooth muscles in the lymphatic vessels to decrease lymph production and flow.[10] When medical management fails, minimally invasive image-guided intervention and surgical intervention are needed.[9] Image-guided embolization of the TD is an effective treatment for postoperative chylothorax[9] and is currently the initial procedure of choice. TD and/or channel embolization is performed by interventional radiologists (Figure 3).[9] Inguinal lymph nodes are accessed under real-time US guidance with a 25-gauge needle and lipiodol is slowly injected.[9] After visualization of the TD and identification of a target lymphatic

https://doi.org/10.37549/JPCR-26-0092

vessel, a 21-gauge-long Chiba needle is placed in the target lymphatic vessel under fluoroscopic guidance.[9] A microcatheter is directed over a guidewire into the lymphatic vessel, and contrast is injected to identify the chylous leak.[9] The TD is embolized on both sides of the lymphatic injury with coils and/or a mixture of cyanoacrylate glue and lipiodol.[9] The minimally invasive approach is successful, with a technical success rate of approximately 70-89% and a clinical success rate of 85-94% in closing the leak.[11]

Conclusion

Injury to the TD leads to the leakage of chyle into the pleural space, causing a chylothorax. The most common cause of chylothorax in children is injury from cardiac surgery when the mediastinum is dissected. It is important to diagnose and localize the chyle leak. Today, INL with MRI is the gold standard for diagnostic imaging and guidance of therapy. Medical management is often the initial therapy. If unsuccessful, image-guided embolization is the initial treatment of choice and is an effective treatment for a persistent chylothorax after unsuccessful medical management.

References

1) Rudrappa M, Pau PM. Chylothorax. In: *StatPearls*. StatPearls Publishing. 2024.

2) McGrath EE. Chylothorax: aetiology, diagnosis and therapeutic options. *Respiratory Medicine*. 2010;104(1):1-8. doi:10.1016/j.rmed.2009.08.010

3) Deso S. Lymphangiography in the diagnosis and localization of various chyle leaks. *Cardiovasc Intervent Radiol*. 2018;35(1):117-126. doi:10.1007/s00270-010-0066-x

4) Fairfax AJ. Chylothorax: a review of 18 cases. *Thorax*. 1986;41(11):880-885. doi:10.1136/thx.41.11.880

5) Shinaoka A, Koshimune S, Suami H, et al. Lower-limb lymphatic drainage pathways and lymph nodes: a CT lymphangiography cadaver study. *Radiology*. 2020;294(1):223-229. doi:10.1148/radiol.2019191169

6) Schwartz FR, James O, Kuo PH, et al. Lymphatic imaging: current noninvasive and invasive techniques. *Semin Intervent Radiol*. 2020;37(3):237-249. doi:10.1055/s-0040-1713441

7) Sugiyama S, Iwai T, Oguri S, Mitsudo K. Ultrasound-guided intranodal lymphangiography with lipiodol as a diagnostic and therapeutic approach for chyle leak after neck dissection. *J Dent Sci*. 2024;19(2):1248-1250. doi:10.1016/j.jds.2023.11.018

8) Lee CW. Postoperative chylothorax: the use of dynamic magnetic resonance lymphangiography and thoracic duct embolization. *Investig Magn Reson Imaging*. 2018;22(3):182. doi:10.13104/imri.2018.22.3.182

9) Shin YR, Lee H, Park Y-H, Park HK. Chylothorax after surgery for congenital cardiac disease: a prevention and management protocol. *Korean J Thorac Cardiovasc Surg*. 2020;53(2):41-48. doi:10.5090/kjtcs.2020.53.2.41

10) Agrawal A, Chaddha U, Kaul V, et al. Multidisciplinary management of chylothorax. *Chest*. 2022;162(6):1402-1412. doi:10.1016/j.chest.2022.06.012

11) Koester TM, Chewning RH, Weldon CB, Shaikh R, Weil BR. Lymphatic embolization for the management of post-operative chyle leaks following solid tumor resection in pediatric patients. *J Pediatr Surg*. 2023;58(11):2141-2148. doi:10.1016/j.jpedsurg.2023.05.016

Pulmonary Aspergilloma

Leah F. Simon, BS; Richard B. Towbin, MD; Carrie M. Schaefer, MD; Alexander J. Towbin, MD

Abstract

Chest CT is the gold standard for diagnosing pulmonary aspergilloma, with key features including a mobile, rounded mass within a pre-existing cavity, typically in the upper lung fields. The Monod sign, characterized by an air crescent surrounding the aspergilloma, is a key diagnostic radiological finding, in addition to cavity wall thickening, that helps distinguish aspergilloma from other cavitary lung pathologies. Chest CT is integral in diagnosis and guiding treatment, determining the need for minimally invasive intervention with direct cavitary antifungal therapy, surgical intervention with lobectomy, or antifungal therapy alone, and monitoring asymptomatic cases or detecting symptom progression over time.

Keywords: chest, lung, infection

Case Summary

A teenaged female with a history of renal transplant developed a cavitary lesion in the right lung positive for *Aspergillus*.

Imaging Findings

Figure 1 shows a frontal chest radiograph indicating consolidation in the right upper lung lobe with several small cavitary areas (arrows) in the upper portion of the consolidation. 5 months prior to obtainining Figures 1, 2, Figure 3 was obtained. In the interval, the cavity was consolidated and enlarged and there was a fungus ball within (arrowheads).

Diagnosis

Pulmonary aspergilloma.

Differential diagnoses for cavitary lung lesions in children encompass various phenotypes of pulmonary aspergillosis, notably invasive pulmonary aspergillosis (IPA) and allergic bronchopulmonary aspergillosis (ABPA). Other pediatric fungal lung diseases with similar presentation include pneumocystis pneumonia, cryptococcal pneumonia, pulmonary histoplasmosis, pulmonary blastomycosis, coccidioidomycosis pneumonia, candida pneumonia, and pulmonary mucormycosis. While there is overlap in radiological and clinical features of these diseases, the presence of a mobile mass within a pre-existing cavity on prone and supine imaging in a relatively asymptomatic, immunocompetent patient is a strong diagnostic indicator of pulmonary aspergilloma.

Discussion

Pulmonary aspergilloma is a noninvasive form of colonization by *Aspergillus* fungi in a pre-existing lung cavity. *Aspergillus* species are ubiquitous environmental fungi that play a role in organic matter decomposition. The most common human pathogens of the species are *A. fumigatus, A. flavus, A. terreus*, and *A. niger*. The pathogenesis involves the inhalation of *Aspergillus* spores, which colonize and multiply within these pre-existing lung cavities, forming a characteristic fungus ball. While daily inhalation of these fungal spores is common, they have the potential to trigger a spectrum of illnesses contingent upon the immune status of the host as well as prior lung pathology.[1]

Aspergillus infection in children spans from benign colonization to

Figure 1. A frontal chest radiograph demonstrating a rounded area of airspace opacification with ill-defined margins and lucencies in the upper aspect of the consolidation (arrows).

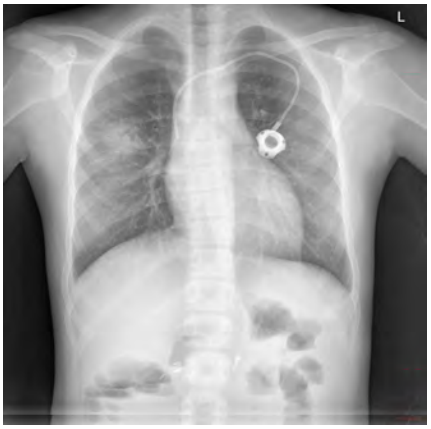

Affiliations: Nova Southeastern University College of Medicine, Fort Lauderdale, Florida (Simon); Department of Radiology, Phoenix Children's Hospital, Phoenix, Arizona (RB Towbin, Schaefer); Department of Radiology, Cincinnati Children's Hospital, University of Cincinnati College of Medicine, Cincinnati, Ohio (AJ Towbin).

Disclosures: The authors have no conflicts of interest to disclose. None of the authors received outside funding for the production of this original manuscript and no part of this article has been previously published elsewhere.

https://doi.org/10.37549/JPCR-26-0093

Figure 2. (A) Axial and (B) coronal images from a chest CT with interval coalescence of the small cavities into a large cavity with an associated fungus ball (arrowheads) within.

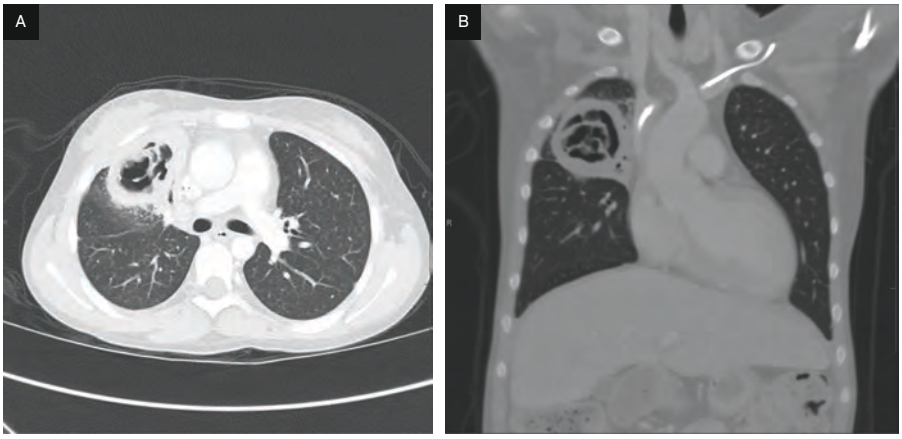

Figure 3. Follow-up frontal chest radiograph showing the sharply defined, round lesion with a large, central cavity.

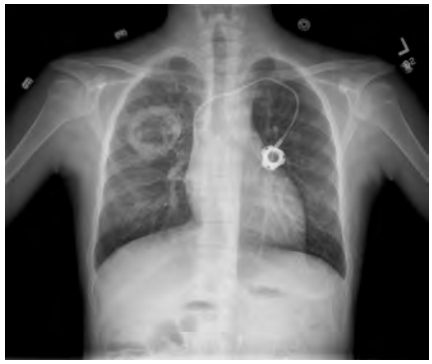

life-threatening invasive diseases. There are 3 broad categories of *Aspergillus*-related pulmonary diseases: ABPA, IPA, and chronic pulmonary aspergillosis (CPA).[2] Pulmonary aspergilloma is under the umbrella of CPA, which encompasses a spectrum of diseases affecting immunocompetent patients with underlying structural pulmonary alteration. Aspergilloma is a less severe form of CPA.[1,3] In immunocompetent children, exposure to *Aspergillus* spores is often inconsequential.[4] However, aspergilloma may develop in cases where cavitary lung lesions or pre-existing lung damage are present, most commonly in cases of tuberculosis or sarcoidosis.[2] Children with immune deficiencies are at a higher risk of developing other forms of aspergillosis, including ABPA, chronic necrotizing aspergillosis, and more severe forms like IPA. ABPA is characterized by hypersensitivity reactions to fungal antigens and typically manifests as an eosinophilic lung disease. This condition primarily occurs in individuals with conditions like long-standing asthma or cystic fibrosis. Invasive aspergillosis, the most severe form of *Aspergillus* infection, is often life-threatening. This condition predominantly affects individuals with compromised immune systems, such as those undergoing immunosuppressive therapies, chemotherapy for malignancies, or organ transplantation.[4]

The clinical presentation of pulmonary aspergilloma primarily revolves around symptoms related to the underlying cavitary lesion and the mechanical effects of the fungus ball. Although patients can be asymptomatic, commonly reported symptoms include hemoptysis, chest pain, cough, and, occasionally, constitutional symptoms such as fever and weight loss. Hemoptysis is a hallmark symptom and can be severe enough to potentially lead to life-threatening bleeding.[5] Hemoptysis in pulmonary aspergilloma is caused by damage to the capillaries within the cavity.[5,6]

Imaging findings are pivotal for the diagnosis of pulmonary aspergilloma. The diagnosis is based on characteristic findings from chest radiographs and CT imaging supported by sputum cultures or the presence of serum antibodies against *Aspergillus*.[7] While chest radiographs may initially appear nonspecific, chest CT is the diagnostic modality of choice. CT scans of the chest unveil distinctive features characteristic of aspergilloma that are instrumental in distinguishing it from other cavitary lung lesions. Typically, chest CT reveals a well-defined, dense, rounded mass within a pre-existing cavity. These masses are frequently located in the upper lobes. Moreover, these masses may display mobility within the cavity in response to changes in the patient's position. One of the characteristic radiological findings is the presence of an air crescent sign surrounding the mass. This sign signifies necrotic lung separating from the wall in an immune-suppressed patient often recovering from IPA. In contrast, the Monod sign represents a mobile fungus ball shifting in a preexisting pulmonary cavity.[1,6,8,9] In addition to these features, the cavity wall may exhibit thickening and irregularities, indicative of chronic inflammation in response to the presence of the fungus ball.[2,6] Importantly, there is usually no evidence of invasion beyond the cavity walls, with the surrounding lung tissue appearing normal.[8]

The treatment of aspergilloma in pediatric patients involves careful consideration of the clinical scenario and underlying conditions. Patients who remain asymptomatic and exhibit stable radiographic findings over extended periods generally do not require any treatment.[5] Repeat CT scans can be used for monitoring if new symptoms arise.[1] Surgical resection, such as lobectomy or segmentectomy, is the most definitive treatment for symptomatic aspergilloma and is often indicated in cases of significant hemoptysis.[2,7] However, surgery carries notable risks and should be

carefully considered based on the child's overall health and pulmonary reserve.[8] In patients unfit for surgery or who refuse an open approach, percutaneous catheter placement into the pulmonary cavity with delivery of amphotericin B is an alternative. Antifungal therapy, typically with agents like itraconazole or voriconazole, may be used as adjunctive treatment when surgery is contraindicated or as a bridge to surgery.[10] In patients with pulmonary hemorrhage, bronchial artery embolization can successfully manage hemoptysis.[3]

Surgical resection is the primary therapy for a pulmonary aspergilloma. The lesion is cured in approximately 80% of cases. Using oral antifungal drugs leads to partial or complete resolution in about 60%. Surgery is often a necessary adjunct. There are insufficient data on the success rate of intracavitary injection of amphotericin B or other antifungal medications. In contrast, patients with invasive aspergillus have a high mortality rate of 30-80%.

Conclusion

Chest CT is the gold standard for diagnosing pulmonary aspergilloma, with key features including a mobile, rounded mass within a pre-existing cavity, typically in the upper lung fields. The Monod sign, characterized by an air crescent surrounding the aspergilloma, is a key diagnostic radiological finding, in addition to cavity wall thickening, that helps distinguish aspergilloma from other cavitary lung pathologies. Chest CT is integral in diagnosis and guiding treatment, determining the need for minimally invasive intervention with direct cavitary antifungal therapy, surgical intervention with lobectomy, or antifungal therapy alone, and monitoring asymptomatic cases or detecting symptom progression over time.

References

1) Pueringer J, Stephens P, Pandya NK, Zaidi S. A case of invasive pulmonary aspergillosis vs. pulmonary aspergilloma in immunocompromised patient with preexisting lung cavity. *Cureus*. 2022;14(8):e28073. doi:10.7759/cureus.28073

2) Panse P, Smith M, Cummings K, et al. The many faces of pulmonary aspergillosis: imaging findings with pathologic correlation. *Radiol Infect Dis*. 2016;3(4):192-200. doi:10.1016/j.jrid.2016.10.002

3) El-Baba F, Gao Y, Soubani AO. Pulmonary aspergillosis: what the generalist needs to know. *Am J Med*. 2020;133(6):668-674. doi:10.1016/j.amjmed.2020.02.025

4) Nitschke A, Sachs P, Suby-Long T, Restauri N. Monod sign. *J Thorac Imaging*. 2013;28(6):W120. doi:10.1097/RTI.0000000000000042

5) Koltsida G, Zaoutis T. Fungal lung disease. *Paediatr Respir Rev*. 2021;37:99-104. doi:10.1016/j.prrv.2020.04.009

6) Russo A, Tiseo G, Falcone M, Menichetti F. Pulmonary aspergillosis: an evolving challenge for diagnosis and treatment. *Infect Dis Ther*. 2020;9(3):511-524. doi:10.1007/s40121-020-00315-4

7) Youssef C, Widlus DM. Imaging diagnosis of aspergilloma. *J Community Hosp Intern Med Perspect*. 2012;2(1):17276. doi:10.3402/jchimp.v2i1.17276

8) Garg M, Bhatia H, Chandra T, et al. Imaging spectrum in chronic pulmonary aspergillosis. *Am J Trop Med Hyg*. 2022;108(1):15-21. doi:10.4269/ajtmh.22-0366

9) Shroff GS, Marom EM, Godoy MCB, Truong MT, Chiles C. CT signs in the lungs. *Semin Ultrasound CT MR*. 2019;40(3):265-274. doi:10.1053/j.sult.2018.11.012

10) Pihlajamaa K, Anttila VJ, Räsänen JV, Kauppi JT, Hodgson U. The fate of aspergilloma patients after surgical treatment-experience from 22 cases. *J Thorac Dis*. 2019;11(10):4298-4307. doi:10.21037/jtd.2019.09.48